15-11-2005

Effects of collective excitations on the quantum well intersubband absorption

X. W. Mi
Chinese Academy of Sciences, Shanghai, China

J. C. Cao
Chinese Academy of Sciences, Shanghai, China

C. Zhang
University of Wollongong, czhang@uow.edu.au

F. B. Meng
Jishou University, China

Effects of collective excitations on the quantum well intersubband absorption

X. W. Mi
College of Physics Science and Information Engineering, Jishou University, Jishou 416000, Hunan, People's Republic of China, and State Key Laboratory of Functional Materials for Informatics, Shanghai Institute of Microsystem and Information Technology, Chinese Academy of Sciences, 865 Changning Road, Shanghai, 200050, People's Republic of China

J. C. Cao[a)]
State Key Laboratory of Functional Materials for Informatics, Shanghai Institute of Microsystem and Information Technology, Chinese Academy of Sciences, 865 Changning Road, Shanghai, 200050, People's Republic of China

C. Zhang
School of Engineering Physics and Institute of Superconducting and Electronic Materials, University of Wollongong, New South Wales 2522, Australia

F. B. Meng
College of Physics Science and Information Engineering, Jishou University, Jishou 416000, Hunan, People's Republic of China

(Received 9 May 2005; accepted 19 October 2005; published online 30 November 2005)

The dependence of the intersubband absorption spectra on the Coulomb interaction and quantum well (QW) width is studied. Rather than following the Fermi–Dirac distribution, we have solved the intersubband equations of motion to determine the subband population self-consistently. We have gone beyond the linear absorption theory to show the effect of various many-body interactions on the absorption spectra. It is found that the redistribution of electrons in excited states reduces the absorption. Our results indicate that the line shape and peak position are determined by the interplay of different collective excitations, such as the Fermi edge singularity and the intersubband plasmon. The dependence of the absorption spectrum on the QW width and the subband effective masses is also discussed. © *2005 American Institute of Physics*. [DOI: 10.1063/1.2137445]

I. INTRODUCTION

The phenomenon of optically induced intersubband transitions (ISBT) in semiconductor quantum wells (QWs) is of great interest to both the condensed matter physics community and the optoelectronics community.[1–6] ISBT in semiconductor QWs are the physical mechanisms for some of the most important technological advances in optoelectronics, such as quantum cascade lasers, quantum well infrared photodetectors, and electro-optical modulators.[2,7–11] ISBT also provide an ideal platform for studying fundamental many-body physics. In a QW structure, the many-body effects in ISBT can be subdivided into the direct and exchange self-energy (XSE) term, the vertex correction term, and the depolarization term caused by the electron plasma. These many-body effects result in various collective excitations, such as the Fermi-edge singularity (FES) and the intersubband plasmon (ISP), which correspond to the vertex correction and the depolarization term. Previous work[2,5,12–18] demonstrated that the intersubband absorption is strongly modified by those collective excitations. It was shown that the depolarization effect can result in intersubband resonance oscillator strength collapsing into a sharp collective mode by using the self-consistent field approach. In order to obtain a better understanding of the many-body effects on the absorption spectra, one must go beyond the mean-field approach, where only ISP is considered. In the formalism based on the Green's function and the density matrix method, both FES and ISP can be modeled on the same footing by including the vertex term. The inclusion of the vertex term leads to a redshift in the absorption peak from that calculated within the mean-field theory. The spectrum peak is between the free-carrier peak and the depolarization-dominated peak, with the spectral shape being dominated by FES. The interplay between FES and ISP significantly changes both the line shape and peak position of the absorption spectrum.[2] In most exiting work, the ground subband population is determined by the Fermi–Dirac distribution, and the first excited subband is assumed to be empty. However, when a QW is driven by an optical field, there are many electrons being excited to the first excited subband that results in electron redistribution. Therefore, it is necessary to consider the electron population in excited subbands by solving the equation of motion self-consistently.

Our purpose in this paper is to study the dependence of the intersubband absorption spectra on the Coulomb interaction and system parameters. These system parameters include subband population, well width, and nonparabolicity of the band structure. By going beyond the linear absorption theory, we have calculated the absorption spectra for InAs and GaAs QWs in the presence of the electron redistribution between subbands. Our main results are (i) when the sub-

[a)]Electronic mail: jccao@mail.sim.ac.cn

band population is determined self-consistently, the absorption rate is significantly reduced; (ii) the intersubband absorption spectra line shape and peak position are determined by ISP and FES; and (iii) the many-body effect on the optical absorption becomes stronger as the QW width decreases. For narrow QWs, the optical absorption is dominated by the FES.

II. MICROSCOPIC THEORETICAL MODEL

The microscopic analysis of coherent effects in photoexcited semiconductors is based on the density matrix theory.[19–21] In the second quantization notation, the Hamiltonian of a multiband system can be written as

$$H = H_0 + H_{\mathrm{Coul}} + H_I, \tag{1}$$

where H_0 is the kinetic energy term,

$$H_0 = \sum_{\mu} \varepsilon_{\mu,\mathbf{k}} a^{+}_{\mu,\mathbf{k}} a_{\mu,\mathbf{k}}. \tag{2}$$

Here $\varepsilon_{\mu,\mathbf{k}}$ is the electron energy, and $a^{+}_{\mu,\mathbf{k}}$, $a_{\mu,\mathbf{k}}$ are the creation and annihilation operators of an electron in the μth subband and with a wave vector $\mathbf{k}$. H_{Coul} is the electron–electron interaction,

$$H_{\mathrm{Coul}} = \frac{1}{2} \sum_{\mu\nu\mu'\nu'\mathbf{k}\mathbf{k}'\mathbf{q}} V^{\mu\nu\nu'\mu'}_{\mathbf{q}} a^{+}_{\mu,\mathbf{k}+\mathbf{q}} a^{\dagger}_{\mu,\mathbf{k}'-\mathbf{q}} a_{\nu',\mathbf{k}'} a_{\mu,\mathbf{k}}, \tag{3}$$

where $V^{\mu\nu\nu'\mu'}_{\mathbf{q}}$ is the Fourier transform of the interaction matrix. The electron–electron interaction is treated within the screened Hartree–Fock approximation; H_I devotes the electron interaction with the optical field. Under the dipole approximation, H_I is written as

$$H_I = -\sum_{\mu,\nu,\mathbf{k}} E_{\mathrm{opt}}(t)(d_{\mu,\nu,\mathbf{k}} a^{+}_{\mu,\mathbf{k}} a_{\nu,\mathbf{k}} + \mathrm{H.c.}),$$

where $d_{\mu,\nu,\mathbf{k}}$ is the optical dipole matrix element. The external optical field, $E_{\mathrm{opt}}(t)$, can be written as

$$E_{\mathrm{opt}}(t) = A_0 \exp(-t^2/\tau^2)\exp(-i\omega t),$$

where τ is the temporal width of the pulse, and ω is the frequency of the external optical field.

The quantities of interest are the electron distribution, $n_{\mu,\mathbf{k}}$, and the intersubband polarization, $p_{\mu,\nu,\mathbf{k}}$. These can be defined as

$$n_{\mu,k} = \langle a^{+}_{\mu,k} a_{\mu,k} \rangle, \tag{4}$$

$$p_{\mu\nu,k} = \langle a^{+}_{\nu,k} a_{\mu,k} \rangle, \tag{5}$$

where $\langle F \rangle$ is the expectation value of operator F. $n_{\mu,\mathbf{k}}$ can also be regarded as the electron population at wave vector $\mathbf{k}$ in the μth subband. $p_{\mu\nu,\mathbf{k}}$ is related to the polarization of the medium, which becomes macroscopic because of the applied external field.

We now derive equations of motion for electron distribution and intersubband polarization. The starting point is the equation of motion in the Heisenberg picture:

$$i\hbar \frac{\partial}{\partial t}\hat{\mathcal{O}} = [\hat{\mathcal{O}}(t), H]. \tag{6}$$

By employing the screened Hartree–Fock approximation with a time-dependent static screening, the final equations of motion can be written as

$$\begin{aligned} i\hbar \frac{\partial n_{1,\mathbf{k}}}{\partial t} = {} & i\hbar \left.\frac{\partial n_{1,\mathbf{k}}}{\partial t}\right|_{\mathrm{col}} - 2i\,\mathrm{Im}[M_{21} E_{\mathrm{opt}}(t) p_{21,\mathbf{k}}] \\ & + \sum_{\mathbf{k}' \neq \mathbf{k}} V^{2112}_{|\mathbf{k}-\mathbf{k}'|}(p_{21,\mathbf{k}'} p^{*}_{21,\mathbf{k}} - p^{*}_{21,\mathbf{k}'} p_{21,\mathbf{k}}) \\ & - V^{2121}_{0} \sum_{\mathbf{k}'} (p_{21,\mathbf{k}'} p^{*}_{21,\mathbf{k}} - p^{*}_{21,\mathbf{k}'} p_{21,\mathbf{k}}), \end{aligned} \tag{7}$$

$$\begin{aligned} i\hbar \frac{\partial}{\partial t} n_{2,\mathbf{k}} = {} & i\hbar \left.\frac{\partial n_{2,\mathbf{k}}}{\partial t}\right|_{\mathrm{col}} + 2i\,\mathrm{Im}[M_{21} E_{\mathrm{opt}}(t) p_{21,\mathbf{k}}] \\ & - \sum_{\mathbf{k}' \neq \mathbf{k}} V^{2112}_{|\mathbf{k}-\mathbf{k}'|}(p_{21,\mathbf{k}'} p^{*}_{21,\mathbf{k}} - p^{*}_{21,\mathbf{k}'} p_{21,\mathbf{k}}) \\ & + V^{2121}_{0} \sum_{\mathbf{k}'} (p_{21,\mathbf{k}'} p^{*}_{21,\mathbf{k}} - p^{*}_{21,\mathbf{k}'} p_{21,\mathbf{k}}), \end{aligned} \tag{8}$$

$$\begin{aligned} i\hbar \frac{\partial}{\partial t} p_{21,\mathbf{k}} = {} & i\hbar \left.\frac{\partial p_{21,\mathbf{k}}}{\partial t}\right|_{\mathrm{col}} + (\varepsilon_{2,\mathbf{k}} - \varepsilon_{1,\mathbf{k}}) p_{21,\mathbf{k}} + M_{21} E_{\mathrm{opt}}(t) \\ & \times (n_{2,\mathbf{k}} - n_{1,\mathbf{k}}) + \Bigg(\sum_{\mathbf{k}' \neq \mathbf{k}} V^{1111}_{|\mathbf{k}-\mathbf{k}'|} n_{1,\mathbf{k}'} \\ & + \sum_{\mathbf{k}' \neq \mathbf{k}} V^{1212}_{|\mathbf{k}-\mathbf{k}'|} n_{2,\mathbf{k}'} \Bigg) p_{21,\mathbf{k}} - \Bigg(\sum_{\mathbf{k}' \neq \mathbf{k}} V^{2222}_{|\mathbf{k}-\mathbf{k}'|} n_{2,\mathbf{k}'} \\ & + \sum_{\mathbf{k}' \neq \mathbf{k}} V^{2121}_{|\mathbf{k}-\mathbf{k}'|} n_{1,\mathbf{k}'} \Bigg) p_{21,\mathbf{k}} \\ & + \sum_{\mathbf{k}' \neq \mathbf{k}} V^{2112}_{|\mathbf{k}-\mathbf{k}'|} p_{21,\mathbf{k}'} (n_{2,\mathbf{k}} - n_{1,\mathbf{k}}) \\ & - \sum_{\mathbf{k}'} V^{1212}_{0} p_{21,\mathbf{k}'} (n_{2,\mathbf{k}} - n_{1,\mathbf{k}}). \end{aligned} \tag{9}$$

In the above equations, the collision terms are $\partial\hat{\mathcal{O}}/\partial t|_{\mathrm{col}} = -\gamma_{\mathrm{col}}\hat{\mathcal{O}}$. Here γ_{col} is the total collision rate, which includes contributions due to electron phonon scattering, electron impurity interactions, etc. It is a rather difficult and complex task to calculate the full energy- and momentum-dependent total collision rate. For the present problem, it is sufficient to treat these incoherent scattering terms by introducing phenomenological decay and dephasing constants to the equations. These equations can then be solved by the fourth-order Runge–Kutta method, subject to the condition of carrier number conservation.

We obtain the total polarization function $P(t)$,

$$P(t) = \frac{1}{4\pi^2 \mathcal{A}} \sum_{\mu \neq \nu} \int d\mathbf{k}\, d^{*}_{\mu\nu,\mathbf{k}} p_{\mu,\nu,\mathbf{k}}, \tag{10}$$

with $\mathcal{A}$ the quantization area of the QW. The absorption coefficient is defined as

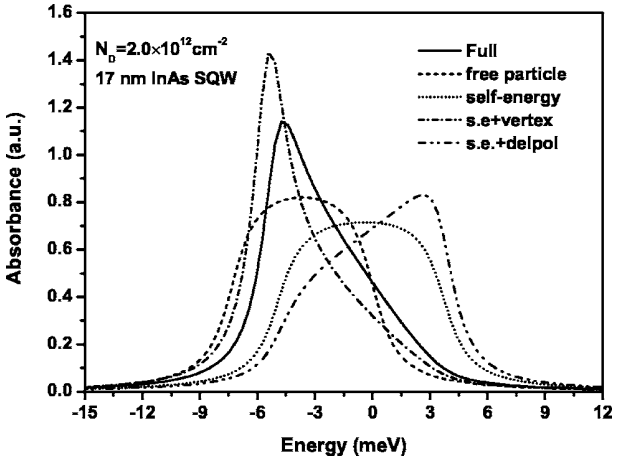

FIG. 1. Intersubband absorption at 12 K and electron density of $N=2.0\times10^{12}$ cm^{-2} for different fictitious scenarios when certain contribution(s) of the Coulomb interaction are excluded.

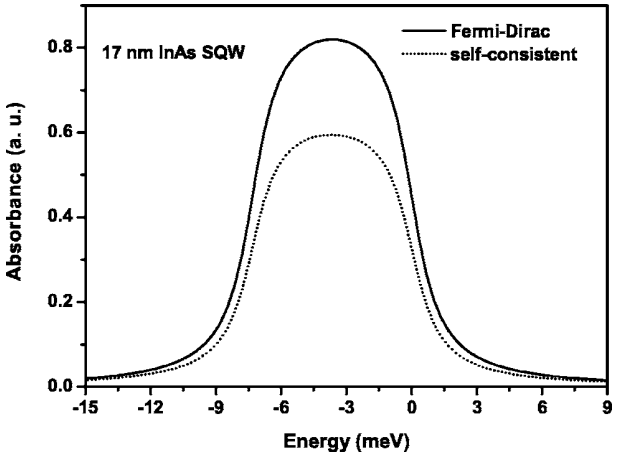

FIG. 2. Intersubband absorption of the free carrier for InAs QW when the subband population is calculated by Fermi–Dirac approximation and solving the intersubband motion equations self-consistently, respectively. Here, the environment temperature is 12 K and the electron density or the initial electron density are 2.0×10^{12} cm^{-2}.

$$\alpha(\omega)=\frac{2\omega}{\epsilon_0\sqrt{\epsilon_b}c}\mathrm{Im}[\chi(\omega)], \tag{11}$$

with ϵ_b the background dielectric constant and c the speed of light in vacuum. Here $\chi(\omega)=P(\omega)/E(\omega)$ is the electron susceptibility, and $P(\omega)$ and $E(\omega)$ are the Fourier transforms of the polarization function $P(t)$ and of the optical field $E_{\mathrm{opt}}(t)$.

III. NUMERICAL RESULTS

In our simulations, we only consider two subbands, the ground and first excited subbands. We choose InAs and GaAs to represent semiconductors with strong and weak nonparabolicity. The material parameters for typical QW structures are $m_1=0.027m_0$, $m_2=0.039m_0$, $\epsilon_b=15.7$, $\gamma_{\mathrm{col}}=1$ meV for InAs QW and $m_1=0.069m_0$, $m_2=0.078m_0$, $\epsilon_b=10.9$, $\gamma_{\mathrm{col}}=1$ meV for GaAs QW. m_0 is the free electron mass. To show how each individual many-body effect influences the absorption spectrum, we calculate the absorption spectrum for different fictitious scenarios when a certain contribution of the Coulomb interaction is included in the calculation. Specifically we consider five cases, which are *free carrier*, *exchange self-energy*, s.e. +vertex, s.e.+depolarization, and *Full* term.

In order to compare our results with those obtained by other groups, we first consider the case in which the subband population is determined by the Fermi–Dirac distribution function. In both Fig. 1 and Fig. 2, the width of QW is 17 nm, and the electron density is $N=2.0\times10^{12}$ cm^{-2}. The intersubband absorption spectra including different many-body effects are shown in Fig. 1. Our result is in agreement with that of recent simulations.[22] The free-carrier absorption curve is very broad and with a flat top. This is the result of the two-dimensional (2D) density of states and the degenerate nature of high-density electron gases. The former leads to a sharp drop of the absorption at the high-energy end, while the latter leads to a similar drop at the lower end. The wide spectrum and the flat top are the result of the Pauli exclusion principle.[22] The XSE effect broadens the free-carrier curve slightly and moves this curve farther up to a higher-energy region. This is because of the reduction of the energy of the heavily populated ground subband, while the almost empty first excited subband is unchanged. When the depolarization effect is included, the absorption spectrum is narrowed and greatly distorted. The peak is also blueshifted, as shown by the dot-dot-dashed curve. The depolarization effect is the result of ISP, a collective excitation in intersubband optics. In comparison to the depolarization effect, the effect due to the vertex term is even more remarkable. With the inclusion of the vertex term, the absorption spectrum shows a significant narrowing and downward shifting, as shown by the dot-dashed curve. This feature is closely related to FES and it indicates an important collective excitation due to the strong correlation of the degenerate electrons. Finally, the solid line represents the effects of all the first-order Coulomb terms. We notice that this curve bears no resemblance to the free-carrier result. The absorption spectrum is completely dominated by the many-body effects. Furthermore, the solid curve is quite similar to the dot-dashed curve, which shows strong features of the FES. What we see here is an interplay of two collective excitations, the FES and the ISP.

In Fig. 1, we assume that the distribution of the electron is determined by the Fermi–Dirac distribution function. This assumption is reasonable only when the bandgap between the ground and the first excited subband is sufficiently large. In this case, most electrons are located in the ground subband and the first excited subband is nearly empty. In general, when the QW is excited by the external optical field, the redistribution of electrons will occur. Some electrons are excited to the first excited subband. Therefore, it is necessary to calculate the distribution of the electron self-consistently. In order to compare the different optical absorption obtained using different electron distributions, the free-carrier optical absorption is calculated and the results are shown in Fig. 2. We can see that the shape of two curves are almost the same. However, the strength of optical absorption when the electron distribution is determined self-consistently is much weaker than that when the electron distribution is determined

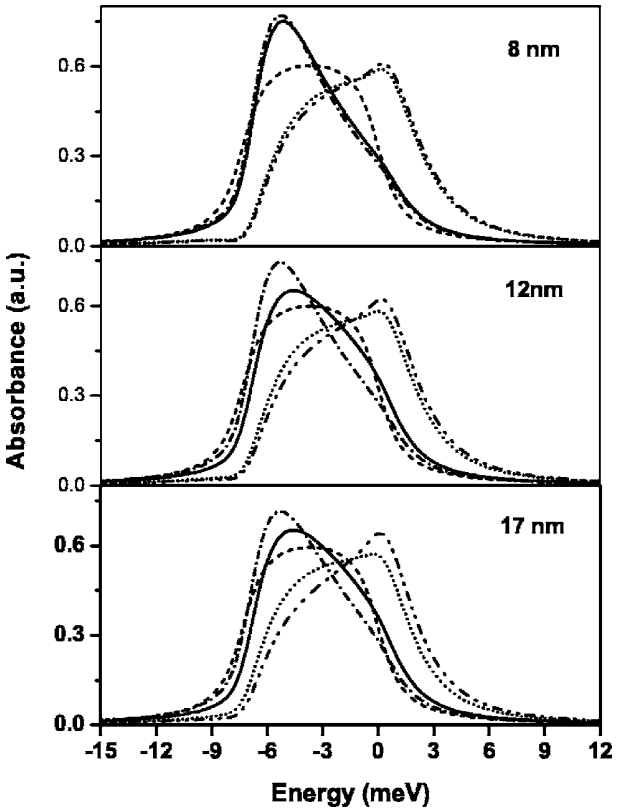

FIG. 3. Intersubband absorption for different width InAs QW. The subband population is calculated self-consistently. Solid lines: full many-body effects; short dashed lines: free-carrier; dotted lines: self-energy; dot-dashed lines: s.e.+vertex; dot-dot-dashed: s.e.+depolarization.

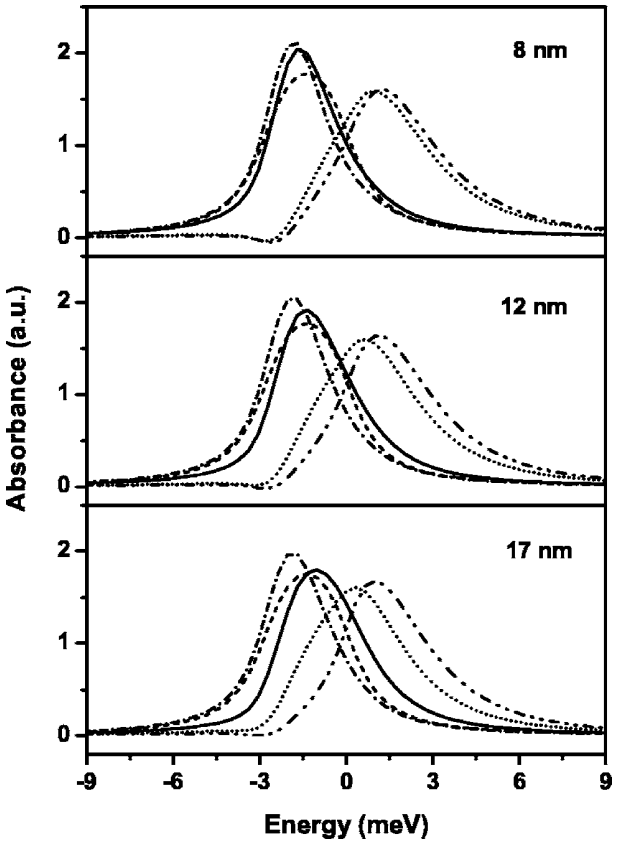

FIG. 4. Intersubband absorption for different width GaAs QW. The subband population is calculated self-consistently. Solid lines: full many-body effects; short dashed lines: free-carrier; dotted lines: self-energy; dot-dashed lines: s.e.+vertex; dot-dot-dashed lines: s.e.+depolarization.

by the Fermi–Dirac distribution. When the redistribution of the electron population takes place, the distribution in the ground state (f_0) decreases and the distribution in the excited state (f_1) increases. Therefore the phase space for optical processes, $f_0(1-f_1)$, is significantly reduced.

Figure 3 shows the intersubband absorption spectra of InAs QW with different well widths of 17, 12, and 8 nm. The distribution of electrons is determined self-consistently by the intersubband equations of motion. The optical absorption flatform completely vanishes and the line shape twists when the XSE effect is included. At the same time, the XSE effect leads to a blueshift of the absorption peak in the absorption spectra. This is due to the modification of the 2D density of states caused by the subband population redistribution. Inclusion of the depolarization effect enhances this trend and a broad absorption peak showed up in the intersubband absorption spectra. If the vertex term is included, the absorption spectra move to the low-energy end. The full absorption spectrum is completely dominated by FES. It should also be noted that the absorption spectra calculated using the self-consistent electron distribution contain more features of ISP. It can be seen that the many-body effect on the optical absorption becomes stronger as the well width decreases. When QW width is reduced to 12 nm, the character due to the depolarization effect increases and the character due to the vertex effect decreases. When the QW width is further reduced to 8 nm, the curves of the self-energy term and the depolarization term almost overlap. At the same time, the curve of the full many-body effect is quite close to the curve of the vertex term. The result is consistent with the understanding that the many-body effect becomes more important in reduced dimensionality.

In order to study the dependence of the intersubband absorption spectra on the difference of the subband effective masses, the intersubband spectra for GaAs QW with weak nonparabolicity are investigated. The result is shown in Fig. 4. The QW widths are 17,12, and 8 nm. When the QW width is 17 nm, the intersubband spectra of the free carrier are dominated by the absorption peak and the line shape shows the Lorentzian curve feature. This can be explained in terms of the reduction in the subband effective masses. Adding certain contribution of the Coulomb interaction and changing the QW width, the intersubband spectra vary in a similar fashion to that of InAs QW, as shown in Fig. 3. It indicates that the intersubband absorption spectra is dominated by the FES feature in GaAs QW.

In conclusion, we presented a microscopic theoretical approach to intersubband optical transitions. Our results are based on the intersubband motion equations in which the subband population is determined self-consistently. We show that the line shape and peak position of the intersubband absorption spectra are the results of the interplay of various many-body effects. The QW width and the subband effective masses can also significantly alter the line shape and peak position of the spectra.

ACKNOWLEDGMENTS

This work is supported by the National Fund for Distinguished Young Scholars of China (Grant No. 60425415), the major project of the National Science Foundation of China (Contract No. 10390162), the Shanghai Municipal Commission of Science and Technology (Contract No. 03JC14082), and the Australian Research Council (Linkage-international scheme).

[1]D. Nikonov, A. Imamoğlu, L. V. Butov, and H. Schmidt, Phys. Rev. Lett. **79**, 4633 (1997).
[2]J. Li and C. Z. Ning, Phys. Rev. Lett. **91**, 097401 (2003).
[3]J. Li and C. Z. Ning, Phys. Rev. Lett. **93**, 087402 (2004).
[4]C. Z. Ning, Phys. Rev. Lett. **93**, 187403 (2004).
[5]C. W. Lou, K. Reimann, M. Woerner, T. Elsaesser, R. Hey, and K. H. Ploog, Phys. Rev. Lett. **92**, 047402 (2004).
[6]J. C. Cao, H. C. Liu, and X. L. Lei, Phys. Rev. B **61**, 5546 (2000).
[7]H. C. Liu and F. Capasso, in *Intersubband Transitions in Quantum Wells: Physics and Device Application I, Vol. 62 of Semiconductors and Semimetals* (Academic, San Diego, 2000).
[8]K. K. Choi, *The Physics of Quantum Well Infrared Photodetectors* (World Scientific, River Edge, NJ, 1997).
[9]S. G. Carter, V. Ciulin, M. S. Sherwin, M. Hanson, A. Huntington, L. A. Coldren, and A. C. Gossard, Appl. Phys. Lett. **84**, 840 (2004).
[10]J. C. Cao, Phys. Rev. Lett. **91**, 237401 (2003).
[11]J. C. Cao and X. L. Lei, Phys. Rev. B **59**, 2199 (1999).
[12]A. Załuzny, Phys. Rev. Lett. **63**, 1633 (1991).
[13]J. C. Ryan, Phys. Rev. B **43**, 12406 (1991).
[14]S. L. Chuang, M. S. C. Luo, S. Schmitt-Rink, and A. Pinczuk, Phys. Rev. B **46**, 1897 (1992).
[15]G. Gumbs, D. Huang, and J. P. Loehr, Phys. Rev. B **51**, 4321 (1995).
[16]R. J. Warburton, C. Gauer, A. Wixforth, and J. P. Kotthaus, Phys. Rev. B **53**, 7903 (1996).
[17]R. J. Warburton, K. Weilhammer, J. P. Kotthaus, M. Thomas, and H. Kroemer, Phys. Rev. Lett. **80**, 2185 (1998).
[18]T. Ando, A. B. Fowler, and F. Stern, Rev. Mod. Phys. **54**, 437 (1982).
[19]T. Kuhn, in *Theory of Transport Properties of Semiconductor Nanostructures*, edited by E. Schöll (Chapman and Hall, London, 1998), Chap. 10.
[20]B. H. Wu and J. C. Cao, J. Phys.: Condens. Matter **16**, 3411 (2004).
[21]X. W. Mi, J. C. Cao, and C. Zhang, J. Appl. Phys. **95**, 1191 (2004).
[22]Jianzhong Li, K. I. Kolokolov, and C. Z. Ning, Proc. SPIE **4986**, 225 (2003).